# Supplemental Figure S1 (Related to Figure 1). NSD1 scores as a top target in a CRISPR Cas9 GSK126 resistance screen in RT cell lines.

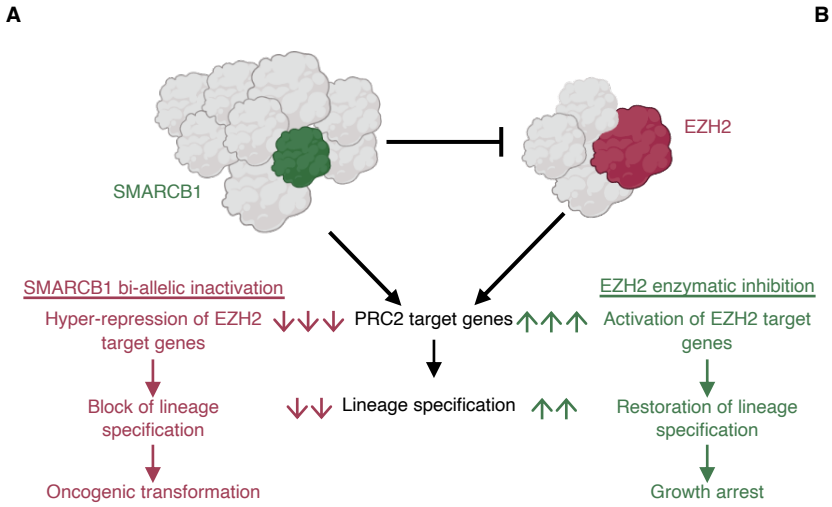


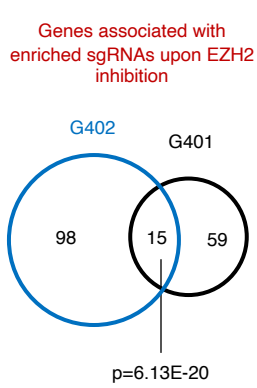


| Gene Symbol | Average LFC |
|---|---|
| TP53* | 9.731195176 |
| RB1* | 3.372002081 |
| KMT2B | 3.319138397 |
| NSD1 | 3.299757043 |

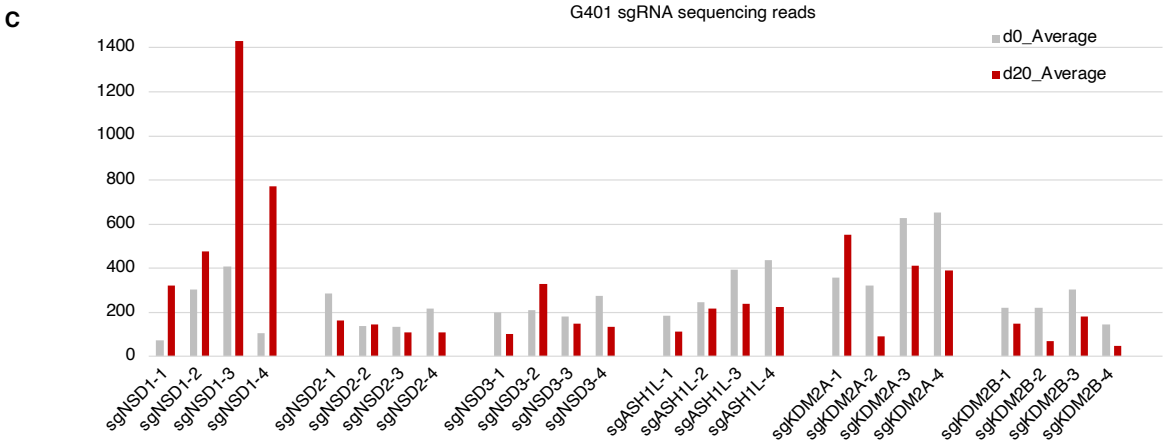


**D**

**G401**

| Gene Symbol | Average LFC | Average -log(p-values) | # of perturbations |
|---|---|---|---|
| **NSD1** | **3.299757043** | **5.209569469** | **4** |
| NSD2 | -0.966702818 | 0.456966716 | 4 |
| NSD3 | -0.839495143 | 0.490327468 | 4 |
| ASH1L | -0.958434082 | 0.460791951 | 4 |
| KDM2A | -1.28021348 | 0.524192312 | 4 |
| KDM2B | -1.722010143 | 0.785594183 | 4 |

**E**

**G402**

| Gene Symbol | Average LFC | Average -log(p-values) | # of perturbations |
|---|---|---|---|
| **NSD1** | **0.532313076** | **2.79335316** | **4** |
| NSD2 | -0.051329955 | 0.612185507 | 4 |
| NSD3 | -0.31863306 | 0.903478576 | 4 |
| ASH1L | -0.096407228 | 0.495013649 | 4 |
| KDM2A | -0.676878809 | 2.209377095 | 4 |
| KDM2B | -0.258744367 | 0.736922859 | 4 |

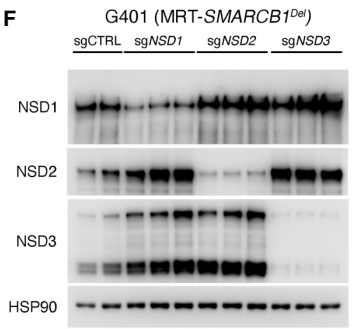


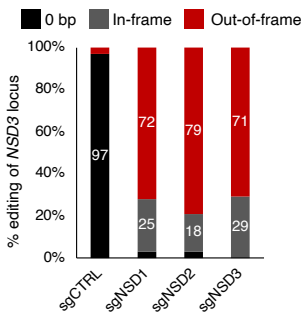


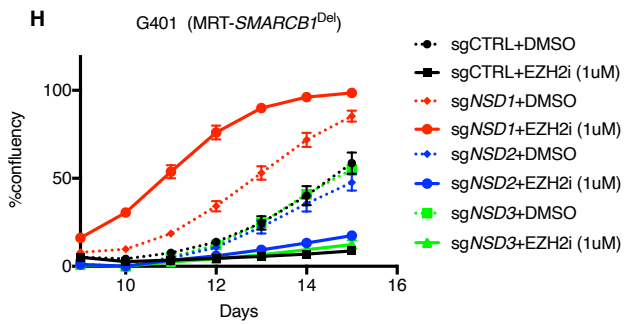


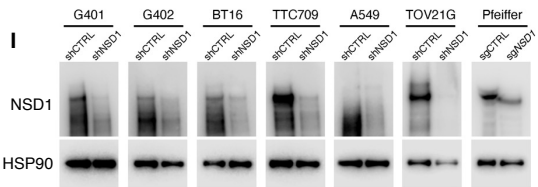

**Supplemental Figure S1. NSD1 scores as a top target in a CRISPR Cas9 GSK126 resistance screen in RT cell lines.**

(A) Schematic overview of the antagonistic relationship between SWI/SNF and EZH2, the action of EZH2 inhibitors and the expected targets from the CRISPR Cas9 GSK126 resistance screen performed in SMARCB1-deficient rhabdoid cell lines.

(B) Venn diagram depicting the number of perturbed genes associated with enriched sgRNAs in G401 and G402 cells.

(C) sgRNA sequencing reads for all genes encoding H3K36me2 writers/erasers in G401 cells at the beginning (d0) and end of the screen (d20).

(D and E) Log2 fold changes of all sgRNAs targeting genes encoding H3K36me2 writers/erasers in the G401 (D) and G402 (E) CRISPR screens.

(F) Immunoblot analysis of the G401 NSD1, NSD2 and NSD3 knockout pools.

(G) Next generation sequencing analysis of the *NSD1*, *NSD2* and *NSD3* loci to assess knockout efficiency. Genes were targeted with sgRNA in G401 cells and genomic DNA sequenced after selection and expansion of the targeted pools (see methods for details). All indels were binned into in-frame, out-of-frame, or 0-bp.

(H) Cell proliferation assay of G401 NSD1/2/3 and control knockout pools

(I) NSD1 knockdown/knockout levels of cell lines used in Figures 1C-F.

Supplemental Figure S2 (Related to Figure 3). NSD1 loss does not affect H3K27me3 removal by EZH2 inhibition

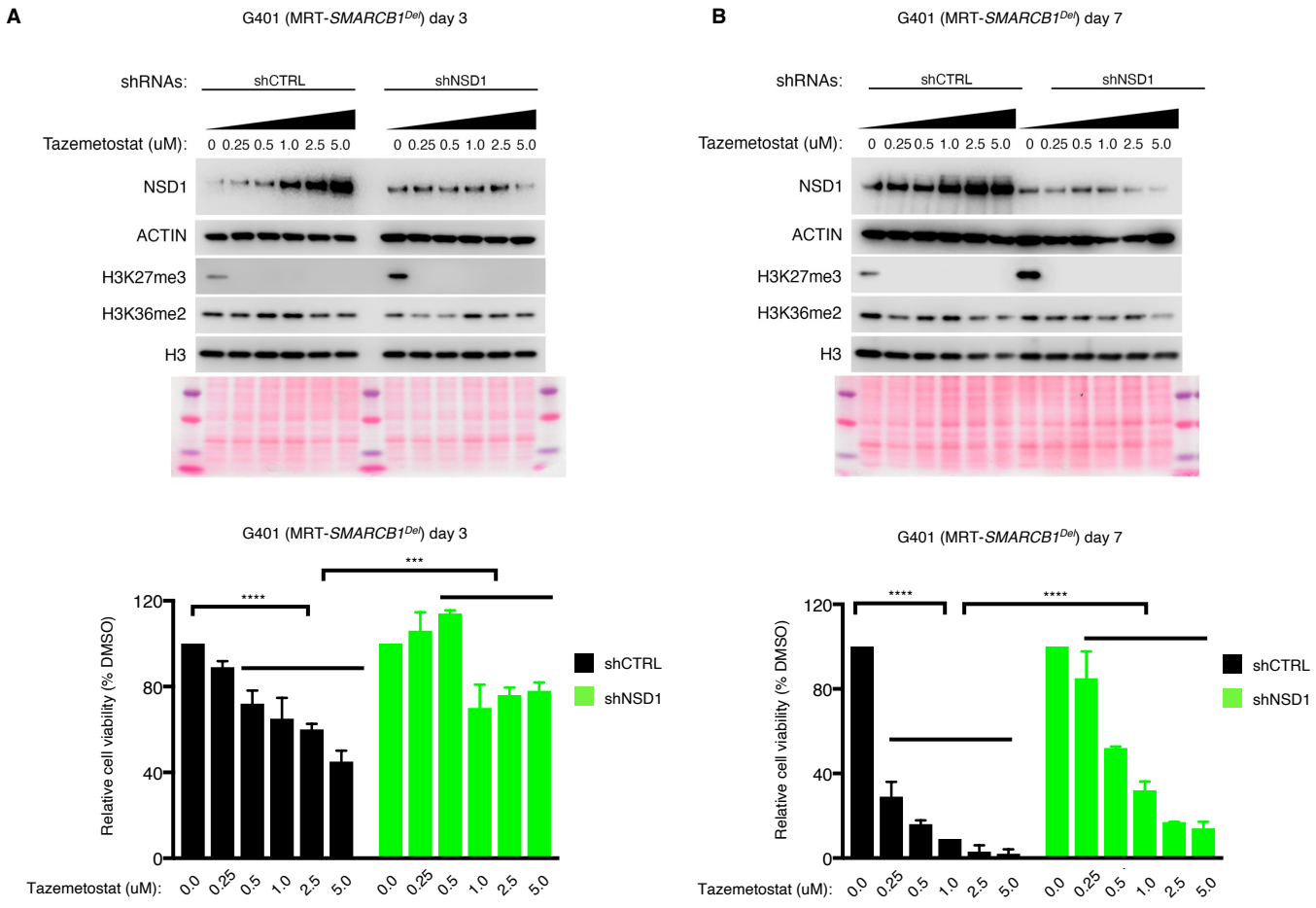

**Supplemental Figure S2. NSD1 loss does not affect H3K27me3 removal by EZH2 inhibition**

(A and B) Immunoblot analysis of control and NSD1 depleted G401 cells treated with various concentration of Tazemetostat and analyzed at days 3 (A) and 7 (B). Viability is calculated for each time point using cell count.

For viability analysis, p values were calculated with Fisher's test. ***: $p<0.001$, ****: $p<0.0001$.

# Supplemental Figure S3 (Related to Figure 3). Mass spectrometry analysis of histone modification changes upon NSD1 KD and EZH2 inhibition

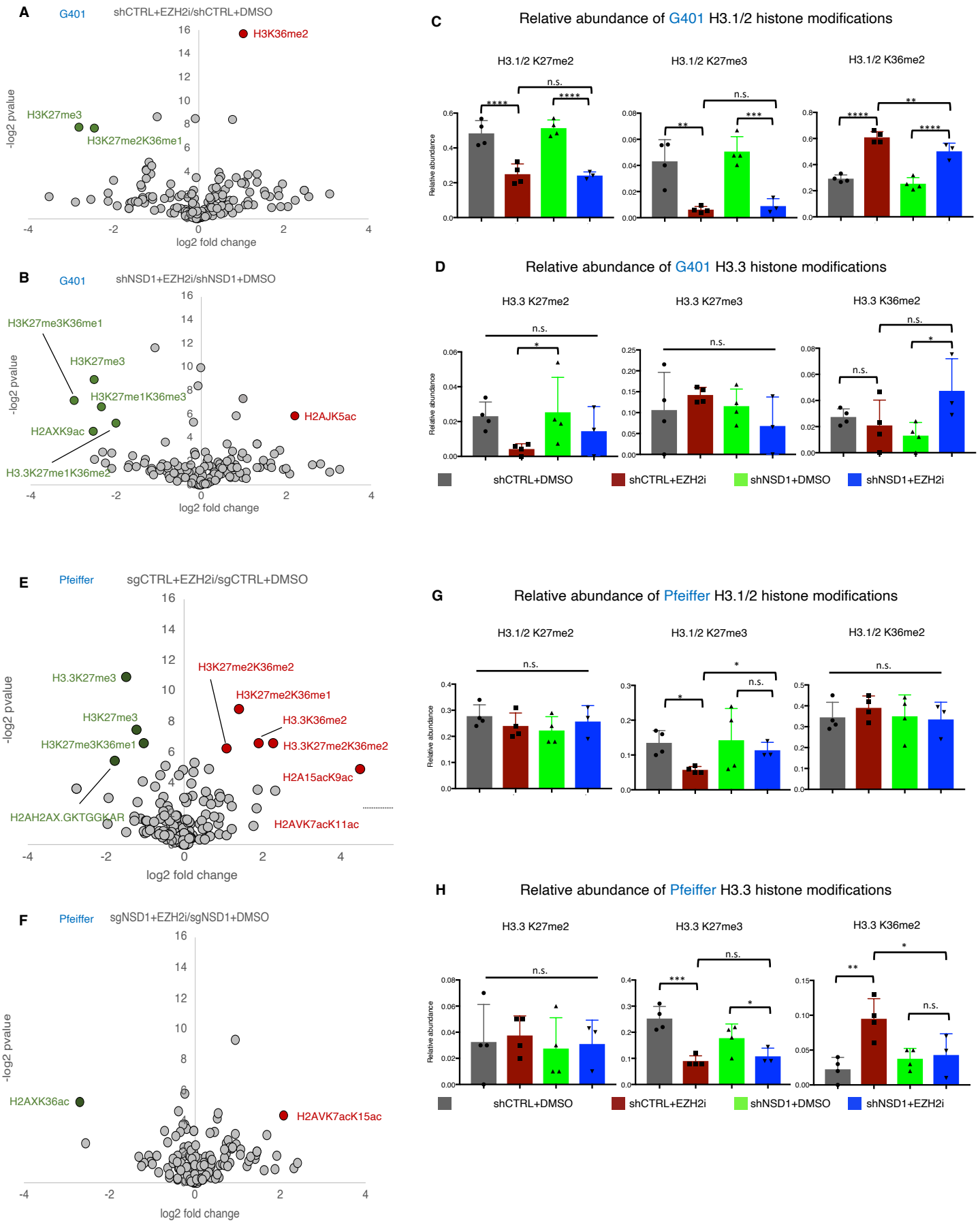

**Supplemental Figure S3. Mass spec analysis of histone modification changes upon NSD1 knockdown and EZH2 inhibition.**

(A-B) Volcano plots of all histone modifications detected in G401 control (A) or NSD1 depleted (B) cells treated with DMSO or 1uM GSK126 for 3 days. The histone modifications that were significantly up or downregulated are marked in the plots with red and green color respectively.

(C-D) Relative abundance of H3K27me2, H3K27me3 and H3K36me2 in G401 H3.1/2 (C) and H3.3 (D) histones after treatment with DMSO or 1uM GSK126 for 3 days

(E-F) Volcano plot of all histone modifications detected in Pfeiffer control (E) or NSD1 depleted (F) cells treated with DMSO or 1uM GSK126 for 3 days. The histone modifications that were significantly up or downregulated are marked in the plots with red and green color respectively.

(G-H) relative abundance of H3K27me2, H3K27me3 and H3K36me2 in Pfeiffer H3.1/2 (G) and H3.3 (H) histones after treatment with DMSO or 1uM GSK126 for 3 days.

For volcano plots, values are considered significant if they have a $p<0.05$ (Student's t-test) and a log2FC>1. For bar graphs, p values are calculated using Fisher's test. *:$p<0.05$, **:$p<0.01$, ***:$p<0.001$.

Supplemental Figure S4 (Related to Figure 3). Differential enrichment analysis of H3K27me3 and H3K36me2 upon NSD1 knockdown and EZH2 inhibition.

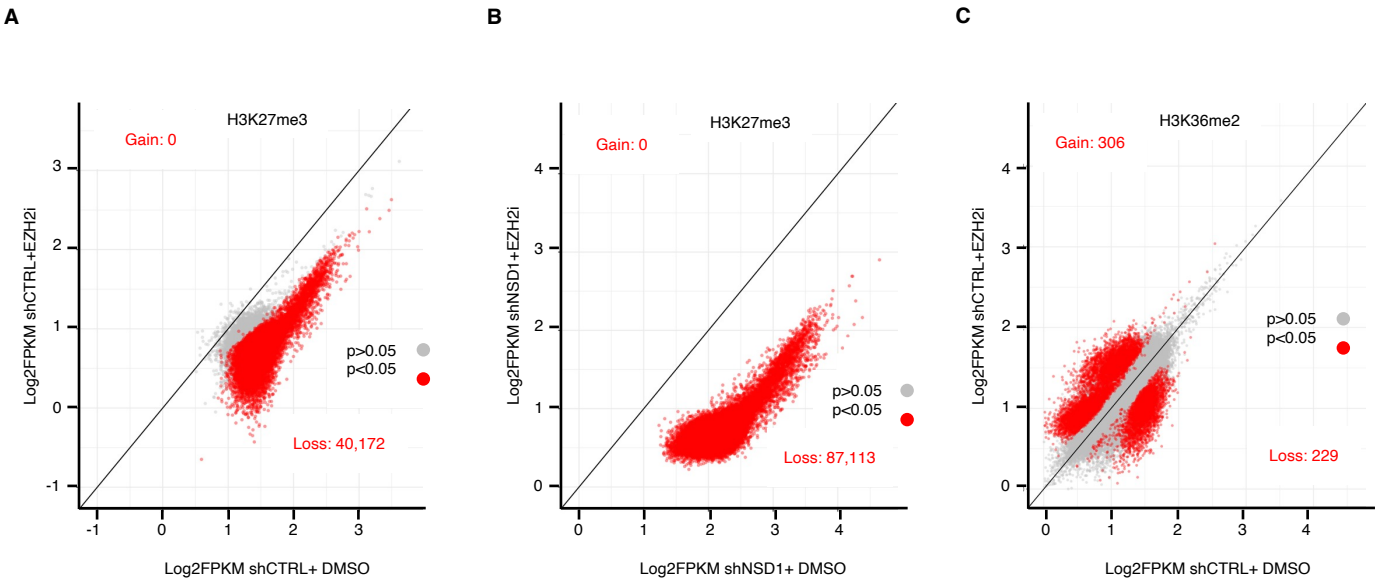

**Supplemental Figure S4. Differential enrichment analysis of H3K27me3 and H3K36me2 upon NSD1 knockdown and EZH2 inhibition.**

(A-B) Scatter plots of regions differentially enriched for H3K27me3 as obtained by ChIP-seq, in control (A) or NSD1 depleted (B) G401 cells treated with 1uM GSK126 for 3 days**.**

(C) Scatter plot of regions differentially enriched for H3K36me2 as obtained by ChIP-seq, in control G401 cells treated with 1uM GSK126 for 3 days**.**

Significance computed using empirical Bayesian statistical tests and linear fitting.

Supplemental Figure S5 (Related to Figure 3). H3K27ac gain upon EZH2 inhibition shows partial dependence on NSD1.

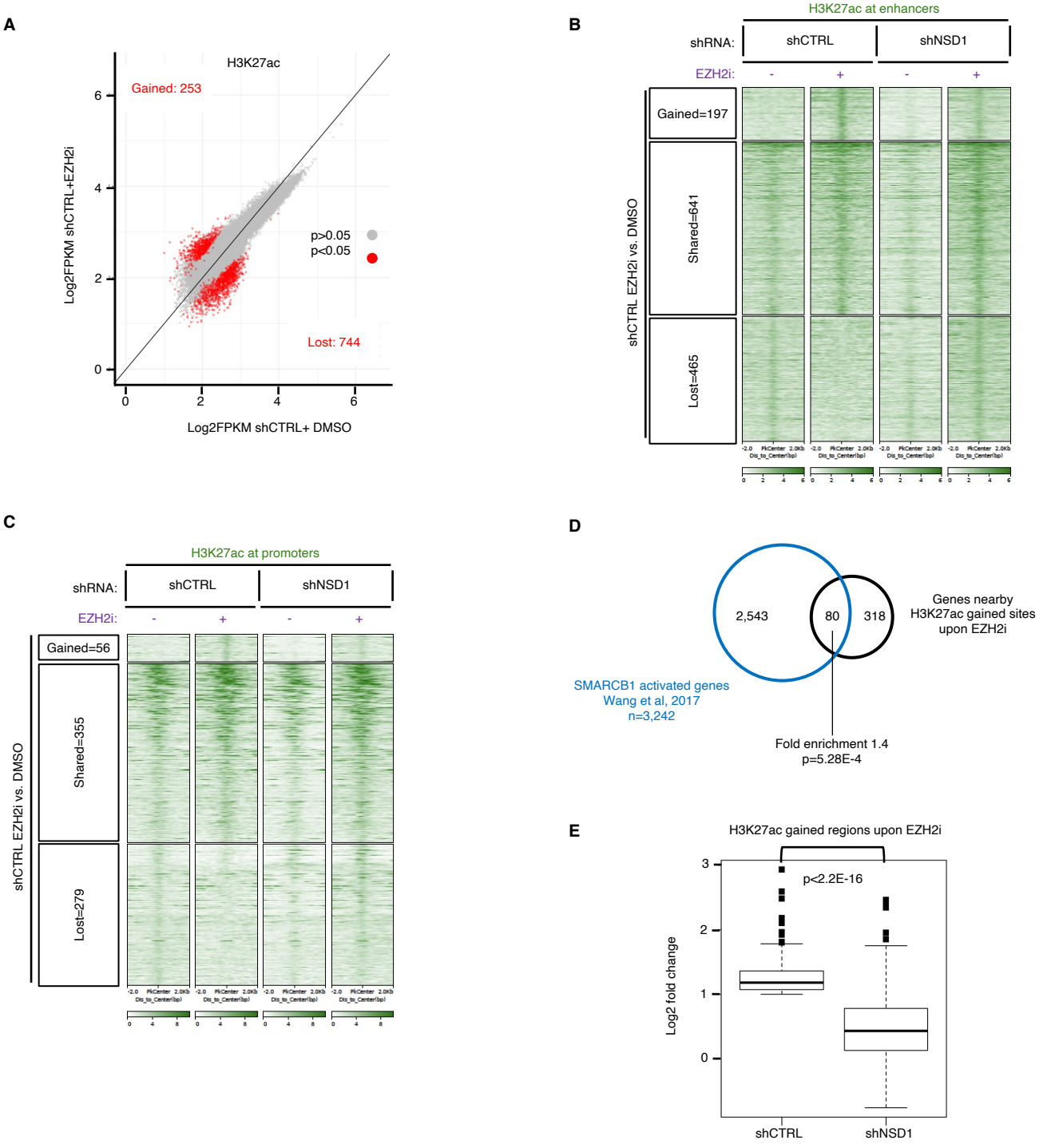

**Supplemental Figure S5. H3K27ac gain upon EZH2 inhibition shows partial dependence on NSD1.**

(A) Scatter plot of the differentially enriched regions for H3K27ac upon NSD1 knockdown in G401 cells, obtained by ChIP-seq. Significance computed using empirical Bayesian statistical tests and linear fitting**.**

(B-C) Heatmaps of enhancers (B) and promoters (C) showing differential H3K27ac enrichment between control and NSD1 depleted cells ranked by gained, shared, and lost H3K27ac signal in control cells treated with 1uM GSK126 for 3 days.

(D) Venn diagram of genes gaining H3K27ac upon EZH2 inhibition, overlapping with genes activated by SMARCB1 in G401 cells. Significance computed using standard Fisher's exact Test.

(E) Box plot of H3K27ac log2FC for the same sites that gain H3K27ac in shCTRL and shNSD1 cells with EZH2 inhibition for the same genomic regions. p value was calculated using Wilcoxon test.

# Supplemental Figure S6 (Related to Figure 5). NSD1 cooperates with SWI/SNF to activate transcription

**A**

| Intersections | Degree | Observed overlap | Expected overlap | Fold enrichment | p value |
|---|---|---|---|---|---|
| EZH2 repressed & SMARCB1 activated | 2 | 317 | 123.65 | 2.56 | 1.73E-64 |
| NSD1 activated & SMARCB1 activated | 2 | 278 | 116.91 | 2.38 | 1.05E-48 |
| NSD1 activated & EZH2 repressed | 2 | 214 | 28.45 | 7.52 | 1.19E-131 |
| NSD1 activated & SMARCB1 activated & EZH2 repressed | 3 | 100 | 4.46 | 22.42 | 1.58E-101 |

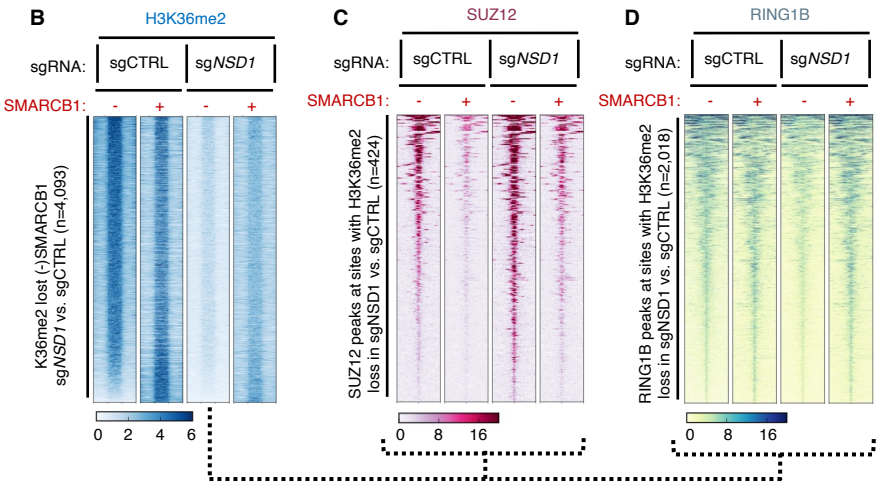


**E**

| Ontology analysis of genes upregulated in G401 (+)SMARCB1 vs. (-)SMARCB1 sgCTRL | FDR |
|---|---|
| system development (GO:0048731) | 8.76E-23 |
| multicellular organism development (GO:0007275) | 2.63E-21 |
| anatomical structure development (GO:0048856) | 3.06E-21 |
| anatomical structure morphogenesis (GO:0009653) | 8.39E-20 |
| developmental process (GO:0032502) | 4.90E-18 |
| animal organ development (GO:0048513) | 2.90E-16 |
| tissue development (GO:0009888) | 4.06E-16 |
| regulation of multicellular organismal process (GO:0051239) | 2.37E-14 |
| regulation of response to stimulus (GO:0048583) | 5.17E-14 |
| multicellular organismal process (GO:0032501) | 1.29E-13 |

G401 cells (rhabdoid tumor)

+SMARCB1 -NSD1

**F**

| Ontology analysis of genes downregulated in G401 sg*NSD1* vs. sgCTRL | FDR |
|---|---|
| anatomical structure development (GO:0048856) | 9.20E-13 |
| developmental process (GO:0032502) | 3.57E-12 |
| system development (GO:0048731) | 4.40E-12 |
| multicellular organism development (GO:0007275) | 1.24E-11 |
| detection of chemical stimulus involved in sensory perception (GO:0050907) | 1.39E-10 |
| movement of cell or subcellular component (GO:0006928) | 4.45E-10 |
| nucleic acid metabolic process (GO:0090304) | 4.88E-10 |
| regulation of localization (GO:0032879) | 9.63E-10 |
| cellular nitrogen compound metabolic process (GO:0034641) | 1.45E-09 |
| regulation of cell communication (GO:0010646) | 1.49E-09 |

Genomic regions spanning genes regulated by SMARCB1 and NSD1

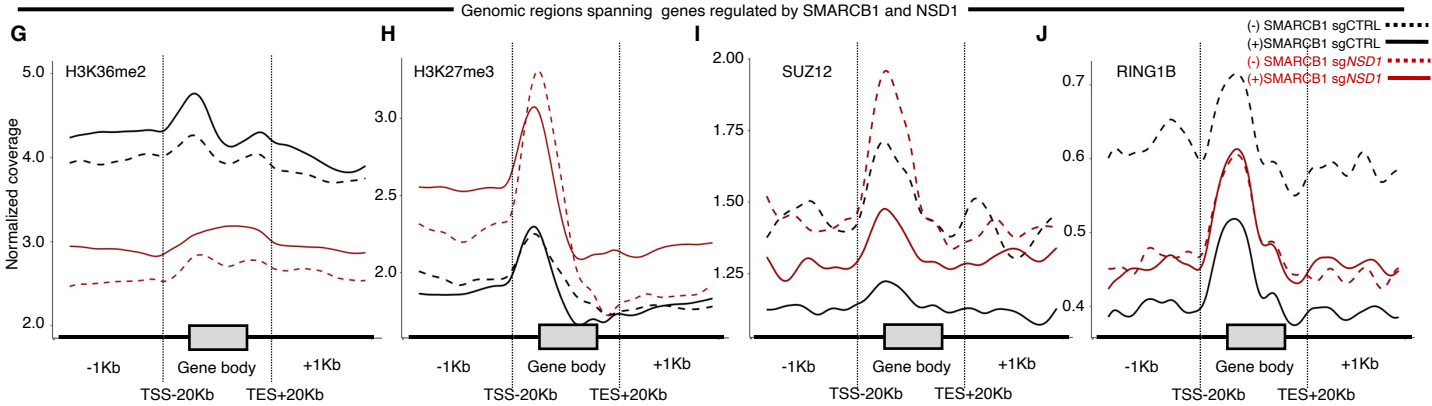


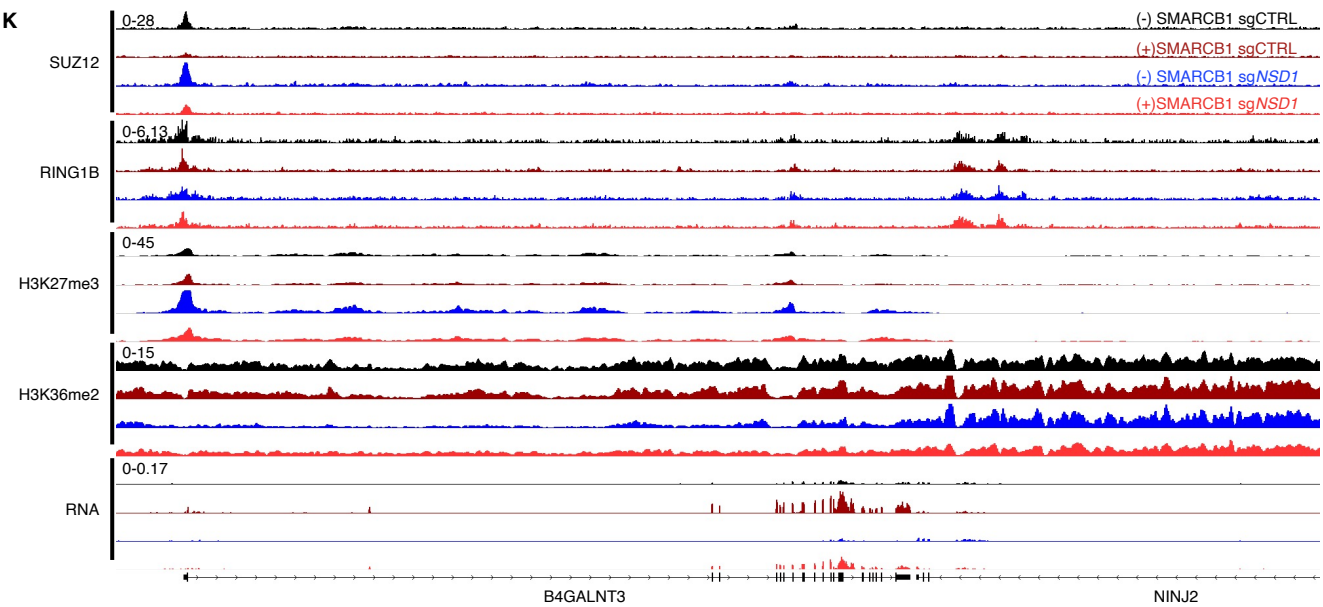

**Supplemental Figure S6. NSD1 cooperates with SWI/SNF to activate transcription.**

(A) Intersection of gene sets displaying p-values (computed using standard Fisher's exact Test for pairwise overlaps and "Exact Test of Multi-set Intersections" for multi-list overlaps) and enrichment statistics (see text for details) for Venn diagram in Figure 5A.

(B) Region-scaled heatmap visualization of H3K36me2 normalized ChIP-seq coverage, rank-ordered based on changes in control vs. NSD1 depleted G401 cells without SMARCB1. Significance computed using empirical Bayesian statistical tests and linear fitting.

(C) Peak centered heatmap visualization of normalized SUZ12 ChIP-Seq coverage, rank-ordered based on changes in H3K36me2 sites lost in sgNSD1 vs sgCTRL, as shown in (B).

(D) Peak centered heatmap visualization of normalized RING1B CUT&RUN coverage, rank-ordered based on changes in H3K36me2 sites lost in sgNSD1 vs sgCTRL, as shown in (B).

(E) Significantly enriched biological processes based on the 977 genes upregulated by SMARCB1 and bound by SMARCC1 (FDR < 0.05 and log2FC > 1).

(F) Significantly enriched biological processes based on the 730 genes downregulated by loss of NSD1.

(G-J) Metaplots of normalized, average coverage for H3K36me2 (G), H3K27me3 (H), SUZ12 (I) and RING1B (J) at +/-20kb of the 289 genes activated by NSD1 and SMARCB1.

(K) Genome browser tracks depicting H3K27me3, H3K36me2, H3K27ac and RNA-seq reads upon SMARCB1 addback in control and NSD1 KO G401 RT cells.

# Supplemental Figure S7 (Related to Figure 5). NSD1 physically interacts with SWI/SNF and PRC1/2 complex members

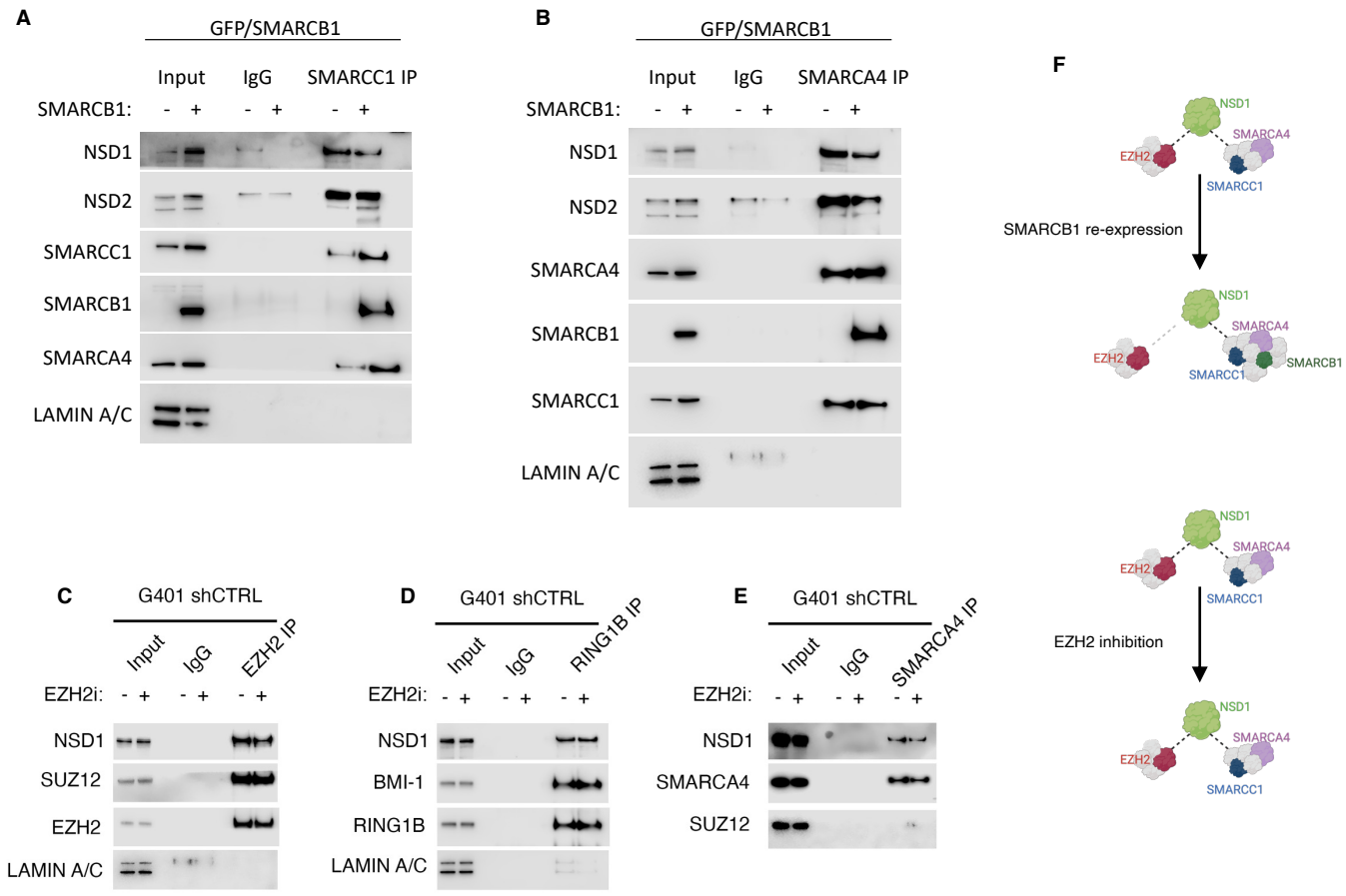

**Supplemental Figure S7. NSD1 physically interacts with SWI/SNF and PRC1/2 complex members.**

(A and B) Co-immunoprecipitation analysis of SWI/SNF core subunits SMARCC1 (A) and SMARCA4 (B) in G401 cells upon SMARCB1 addback.

(C and D) Co-immunoprecipitation analysis of PRC1/2 subunits EZH2-PRC2 (C) and RING1B-PRC1 (D) in G401 cells treated with DMSO or 1uM GSK126 for 3 days.

(E) Co-immunoprecipitation analysis of SWI/SNF ATPase SMARCA4 in G401 cells treated with DMSO or 1uM GSK126 for 3 days.

(F) Schematic representation of the co-IP results.

# Supplemental Figure S8 (Related to Figure 5). NSD1 inactivation co-occurs with SWI/SNF mutations in cancer

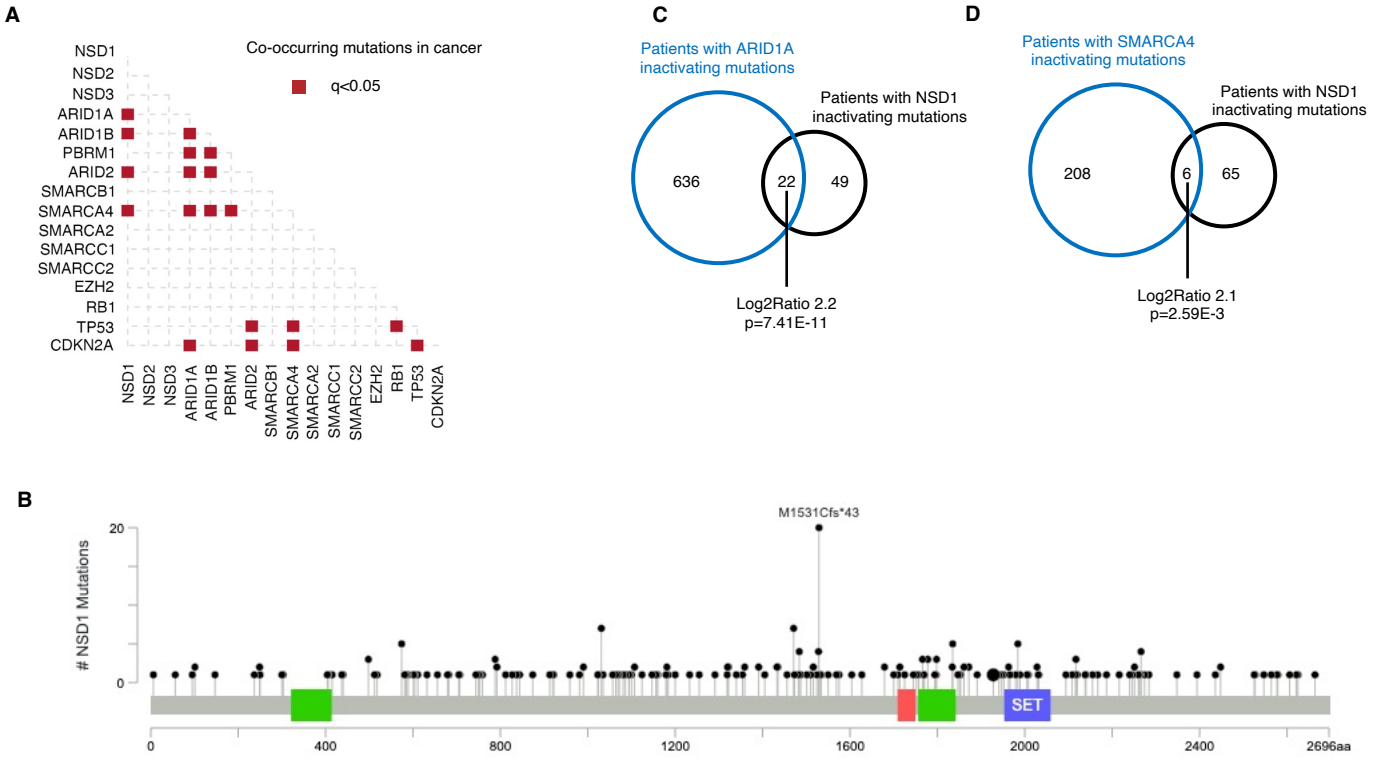

**Supplemental Figure S8. NSD1 and SWI/SNF mutations co-exist in cancer patients.**

(A) Analysis of co-mutation and exclusivity in focused cohort of cancer patients (see methods for details). Fisher's Exact Test (R version 3.4.2) was used for mutational analysis and p values were then corrected for multiple testing by using package "qvalue" (R version 3.4.2).

(B) Pathogenic mutations in *NSD1* gene used for the cBioportal analysis.

(C and D) Venn diagram of cancer samples with NSD1 and ARID1A (C) or SMARCA4 (D) co-occurring mutations in focused analysis. Fisher's Exact Test (R version 3.4.2) was used for mutational analysis and p values were then corrected for multiple testing by using package "qvalue" (R version 3.4.2).